

# Bandpass filters based on $\pi$ -shifted long-period fiber gratings for actively mode-locked erbium fiber lasers

O. Deparis, R. Kiyon, O. Pottiez, and M. Blondel

*Advanced Research in Optics Group, Service d'Electromagnétisme et de Télécommunications, Faculté Polytechnique de Mons, 31 Boulevard Dolez, B-7000 Mons, Belgium*

I. G. Korolev, S. A. Vasiliev, and E. M. Dianov

*Fiber Optics Research Center at General Physics Institute, 38 Vavilov Street, 117756 Moscow, Russia*

Received March 26, 2001

We have fabricated bandpass filters based on  $\pi$ -shifted long-period gratings for application in actively mode-locked erbium fiber lasers. Introducing the  $\pi$ -phase shift in the middle of the grating opens a bandpass within the core-cladding mode resonance peaks. With a 22-nm bandwidth filter inserted in an actively mode-locked erbium fiber sigma laser, solitonlike pulses are generated, with a power-dependent duration of  $\approx 3$ –5 ps, at a 3-GHz repetition rate. These all-fiber filters have the advantages of low insertion loss ( $< 0.5$  dB) and a wide bandwidth (10–20 nm), and they do not require that a circulator be inserted into the laser cavity. © 2001 Optical Society of America

OCIS codes: 060.2340, 140.4050, 140.3500.

Long-period fiber gratings (LPGs) couple light from the fundamental guided mode to forward-propagating cladding modes.<sup>1</sup> Basically, they form low-loss band-rejection filters, which have found applications as gain flatteners for erbium-doped fiber amplifiers and optical sensors. There exist other applications in which LPGs are potentially attractive, but they require bandpass instead of notch filter characteristics. Fortunately, bandpass filters can be built from LPGs as well. By use of a pair of matched LPGs, the cladding can be used as a bypass for the resonant light while the nonresonant light propagating in the core is blocked intentionally.<sup>2</sup> However, the insertion loss of the device reported in Ref. 2 was relatively high. Therefore, besides this elaborate design, one could simply combine two unmatched LPGs, with the central wavelength of the resulting bandpass filter halfway between the LPG resonance wavelengths. In these approaches, two LPGs are needed to define the bandpass. But could a bandpass filter be designed from a single LPG? The solution that we propose here, for what is believed to be the first time, is to introduce a  $\pi$ -phase shift in the middle of the LPG during its fabrication, with the consequence that a bandpass is opened within the core-cladding mode resonance peaks of the LPG. In actively mode-locked erbium fiber lasers, which is the application discussed in this Letter,  $\pi$ -shifted long-period grating (PS-LPG) filters offer advantages in comparison with classical interference filters or fiber Bragg grating filters. Like the former, they provide bandwidth of the order of 10 nm but in an all-fiber low-loss version. Unlike the latter, they do not require that a circulator be inserted into the laser cavity, as they operate in transmission and not in reflection. Moreover, one can also combine PS-LPG filters in series to obtain various filtering characteristics. In this Letter we report on the fabrication of PS-LPG filters, and we demonstrate what we believe to be their first application in actively mode-locked erbium fiber lasers.

Several PS-LPGs with two different lengths (24 mm for grating 1 and 65 mm for grating 2) were fabricated in hydrogen-loaded SMF-28 fiber with a step-by-step technique with a cw frequency-doubled argon-ion laser. Hydrogen loading was performed by heat treatment of the fiber under 120 atm at 100 °C for 12 h. The power density of the focused laser beam was  $\sim 16$  kW/cm<sup>2</sup>. The period of the gratings was 336  $\mu$ m. The UV-induced refractive-index changes were estimated to be  $8 \times 10^{-4}$  and  $3 \times 10^{-4}$  for gratings 1 and 2, respectively. The  $\pi$ -phase shift was obtained by introduction of a nonirradiated fiber section of half-period length into the middle of the grating during fabrication. After writing the grating, we applied additional heat treatment to outdiffuse the remaining hydrogen. Then, hydrofluoric acid etching of the grating<sup>3</sup> was used to tune the positions of the resonance peaks until one of them reached the desired value. The transmission spectra of two PS-LPGs are shown in Fig. 1. The short and long grating lengths resulted in broadband and narrow-band resonance peaks, respectively. Because of the  $\pi$ -phase shift, a bandpass is opened in each core-cladding-mode resonance peak of the grating. The useful resonance peak (for a filter that is designed to operate near 1550 nm) corresponds to coupling between fundamental guide mode HE<sub>11</sub> and radially symmetric cladding modes HE<sub>1m</sub> of orders  $m = 6$  and  $m = 7$  for gratings 1 and 2, respectively. In the wavelength region of interest, the transmission spectra of PS-LPG filters 1 and 2 are shown in Fig. 2. The peak wavelengths of these filters are 1545.5 and 1546.8 nm, respectively, and their transmission bandwidths (FWHM) are 22.0 and 9.7 nm, respectively. The insertion loss of the filters at the resonance wavelength is lower than 0.5 dB. Maximum out-of-band rejection of the filters is approximately 12–13 dB and occurs at two wavelengths that are located symmetrically with respect to the resonance wavelength; the wider the bandpass, the greater the distance between these two wavelengths. On the shorter- and longer-wavelength

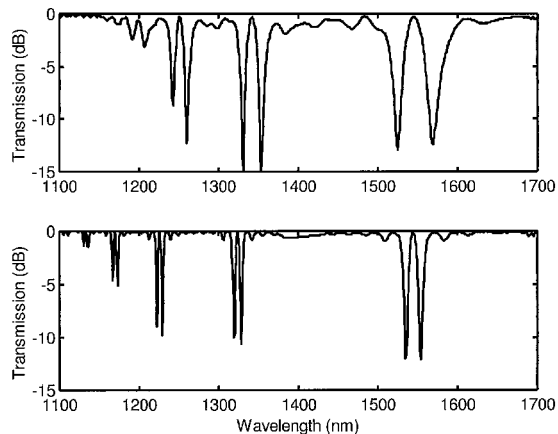


Fig. 1. Transmission spectra of PS-LPGs 1 (top) and 2 (bottom). Note the bandpass in each core-cladding-mode resonance peak, resulting from the  $\pi$ -phase shift introduced in the middle of the LPG.

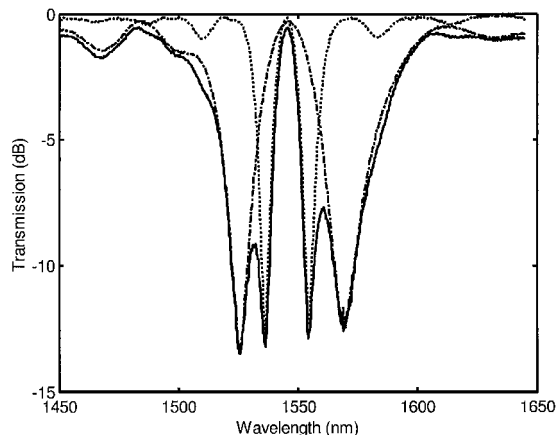


Fig. 2. Transmission spectra of PS-LPGs 1 (dashed-dotted curve) and 2 (dotted curve) and their serial combination 12 (solid curve), measured near the wavelength of interest (1550 nm).

sides of the maximal rejection points, the loss of the filter decreases and tends to zero (as for a classical LPG). Clearly, once the width of the rejection band is imposed, the width of the rejection band is fixed, too. This situation is different if two PS-LPGs with matched central wavelengths but much different bandpass widths are combined in series. In this case the bandpass width is determined by the grating with the narrowest bandpass, and the rejection band is determined by the other grating. The transmission spectrum of the serial combination of gratings 1 and 2 (denoted 12) is shown in Fig. 2. The peak wavelength and the FWHM bandwidth of the resulting filter are 1545.8 and 9.0 nm, respectively, and the insertion loss is  $\sim 0.5$  dB. The usefulness of such a filter is highlighted below.

For our experimental demonstration, we use a stabilized actively mode-locked erbium fiber sigma laser.<sup>4</sup> The sigma configuration<sup>5</sup> is functionally equivalent to a polarization-maintaining (PM) ring cavity. A dispersion-shifted fiber (200 m) in the non-PM section of the sigma laser provides nonlinear

pulse shortening through the formation of soliton-like pulses in the cavity. The fundamental cavity resonance frequency is  $f_c \approx 395$  kHz. The laser is harmonically mode locked at modulation frequency  $f_m \approx 3$  GHz. The PS-LPG filter is spliced into the non-PM section of the sigma cavity. We tested filters 1, 2, and 12 separately inside the laser cavity. In all cases we observed a decrease of the pulse duration by increasing pump power, which means that nonlinear effects were important in the cavity.

With PS-LPG filter 2 inside the cavity, lasing occurs predominantly near 1560 nm and secondarily near 1545 nm, respectively, out of and within the filter bandpass. Lasing could be suppressed at the longer wavelength by an increase of the cavity loss (e.g., by bending of some portion of the fiber). These observations can be explained as follows: In the laser, gain is clamped to cold-cavity loss, which is typically small (estimated to be 7 dB). Therefore, a threshold can be achieved with a low degree of population inversion in the erbium fiber, and the gain profile exhibits its maximum at longer wavelengths, at which the secondary erbium emission peak is located.<sup>6</sup> However, far on either side of the bandpass, the loss of the PS-LPG filter is small (Fig. 2). For filter 2, the loss becomes less than 1 dB at wavelengths higher (lower) than approximately 1560 nm (1530 nm). For this reason, lasing can occur near both 1560 and 1545 nm, where loss is small. When the cold-cavity loss is increased, the laser is forced to operate at near-complete inversion, and the gain profile exhibits its maximum near 1530 nm.<sup>6</sup> As a result, here lasing is favored at the shorter wavelength when loss is increased. With PS-LPG filter 1 or 12 inside the cavity, however, lasing was observed only within the filter bandpass. This is so because, in both cases, rejection of the filter is strong enough that lasing outside the bandpass is avoided. Figure 3 shows optical spectra and autocorrelation traces of the mode-locked pulses obtained with PS-LPG filter 1 inside the cavity, measured at increasing average intracavity power. We estimated the average intracavity power,  $P_{\text{cav}}$ , at the input end of the 20% output coupler by measuring the average output power. The central wavelength of the pulse spectrum (1549.8 nm) is slightly shifted toward longer wavelengths with respect to the central wavelength of the filter. The tendency for lasing at longer wavelengths discussed above is observed here, because the wavelength-dependent loss introduced by the PS-LPG filter is flat on a broad wavelength range (dotted curve in Fig. 3). As the intracavity power is increased, the pulse duration decreases and the pulse spectrum broadens, owing to the soliton effect (note the typical sidebands in the pulse spectrum as a result of periodic perturbations of the solitonlike pulse in the cavity<sup>7</sup>). At  $P_{\text{cav}}$  values of 3.55, 9.70, and 15.65 mW, the pulse FWHM spectral widths (measured) are 0.42, 0.54, and 0.61 nm, respectively, and the pulse FWHM durations (calculated by fitting of the autocorrelation trace, assuming a  $\text{sech}^2$  pulse shape) are 5.6, 4.5, and 3.4 ps, respectively. In all cases, the pulse's time-bandwidth product is  $\approx 0.3$ . Figure 4 shows

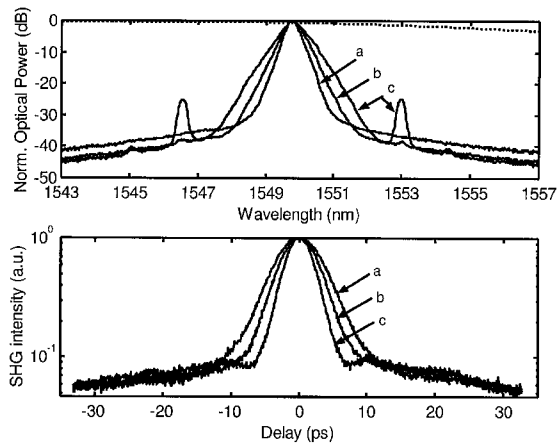


Fig. 3. Optical spectra (top) and autocorrelation traces (bottom) of mode-locked pulses, measured at increasing average intracavity power. a,  $P_{\text{cav}} = 3.55$  mW, b,  $P_{\text{cav}} = 9.70$  mW, and c,  $P_{\text{cav}} = 15.65$  mW. The transmission spectrum of PS-LPG filter 1 that is used in the laser cavity is shown by the dotted curve. SHG, second-harmonic generation.

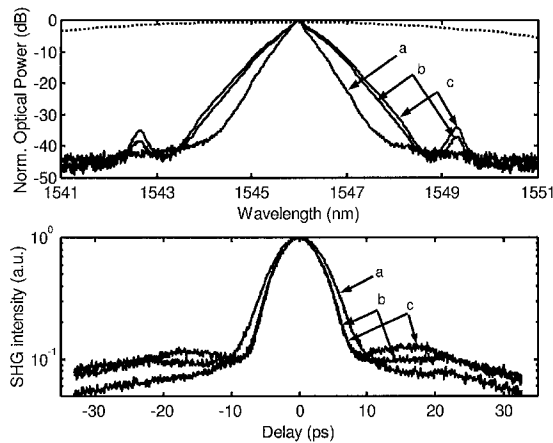


Fig. 4. Optical spectra (top) and autocorrelation traces (bottom) of mode-locked pulses, measured at increasing average intracavity power. a,  $P_{\text{cav}} = 4.50$  mW, b,  $P_{\text{cav}} = 10.25$  mW, and c,  $P_{\text{cav}} = 12.55$  mW. The transmission spectrum of PS-LPG filter 12 that is used in the laser cavity is shown by the dotted curve. SHG, second-harmonic generation.

the optical spectra and autocorrelation traces of the mode-locked pulses obtained with PS-LPG filter 12 inside the cavity, measured at increasing average intracavity power. The central wavelength of the pulse spectrum (1546.0 nm) almost coincides with the central wavelength of the filter. The narrower bandwidth ( $\approx 2.4$  times) of PS-LPG filter 12 in comparison with PS-LPG filter 1 introduces stronger wavelength-dependent loss that prevents the pulse spectrum from shifting to longer wavelengths. Moreover, as is predicted by active-mode-locking theory,<sup>8</sup>

even in the absence of nonlinear effects, a narrower filter bandwidth leads to a longer pulse duration. At  $P_{\text{cav}}$  values of 4.50, 10.25, and 12.55 mW, the pulse FWHM spectral widths are 0.35, 0.44, and 0.52 nm, respectively, and the pulse FWHM durations are 6.1, 5.2, and 5.1 ps, respectively. In all cases, the pulse's time-bandwidth product is  $\approx 0.3$ . Interestingly, we note that at high average intracavity power pedestals appear in the autocorrelation trace that are more pronounced with the narrow-band filter (Fig. 4) than with the broadband filter (Fig. 3). This difference is due to the stronger filtering of the former filter when the pulse spectrum broadens nonlinearly as  $P_{\text{cav}}$  increases. To check the stability of the pulses generated from the laser with the PS-LPG filter, we measured the rf spectrum of the detected pulse train near carrier frequency  $f_m$ . We chose different frequency spans at which to observe relaxation oscillations (located at tens of kilohertz from carrier) and supermodes (separated by the cavity's free spectral range,  $f_c$ ). rf spectrum measurements showed strong damping of relaxation oscillations ( $>70$  dB) and good suppression of supermode noise ( $\approx 45$  dB).

In conclusion, novel bandpass filters based on  $\pi$ -shifted long-period gratings have been fabricated, and their performance has been tested in an actively mode-locked erbium fiber laser for what is believed to be the first time. These all-fiber filters exhibit low insertion loss ( $<0.5$  dB) and do not require that a circulator be used in the laser cavity. Their wide bandwidth (up to 20 nm) is also an advantage because, in actively mode-locked lasers, a wider filter bandwidth naturally leads to shorter pulses, when all other parameters, such as modulation frequency, modulation depth, and cavity loss, are the same.

This work was supported by the Inter-University Attraction Pole program of the Belgian government under grant 4/07. O. Deparis's e-mail address is Deparis@telecom.fpms.ac.be.

## References

1. A. M. Vengsarkar, P. J. Lemaire, J. B. Judkins, V. Bhatia, T. Erdogan, and J. E. Sipe, *IEEE J. Lightwave Technol.* **14**, 58 (1996).
2. D. S. Starodubov, V. Grubsky, and J. Feinberg, *IEEE Photon. Technol. Lett.* **10**, 1590 (1998).
3. S. A. Vasiliev, E. M. Dianov, D. Varelas, H. G. Limberger, and R. P. Salathé, *Opt. Lett.* **21**, 1830 (1996).
4. R. Kiyari, O. Deparis, O. Pottiez, P. Mégret, and M. Blondel, *Opt. Lett.* **24**, 1029 (1999).
5. T. F. Carruthers, I. N. Duling III, and M. L. Dennis, *Electron. Lett.* **30**, 1051 (1994).
6. P. Franco, M. Midrio, A. Tozzato, M. Romagnoli, and F. Fontana, *J. Opt. Soc. Am. B* **11**, 1090 (1994).
7. D. U. Noske, N. Pandit, and J. R. Taylor, *Opt. Lett.* **17**, 1515 (1992).
8. D. J. Kuizenga and A. E. Siegman, *IEEE J. Quantum Electron.* **6**, 694 (1970).